

Magnetic Driving of Gamma-Ray Burst Outflows



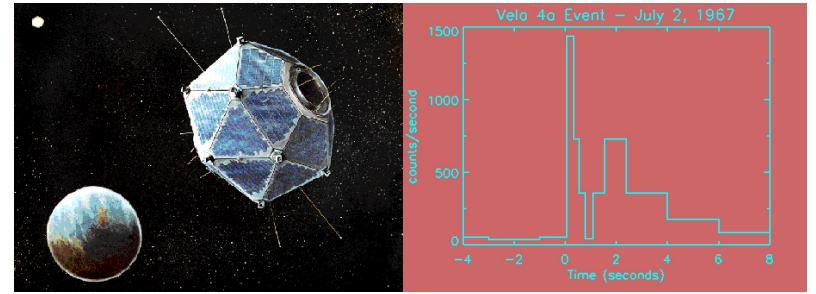
Nektarios Vlahakis
University of Athens

Outline

- GRBs and their afterglows
 - observations
 - our understanding
- the MHD description
 - general theory
 - the model
 - results

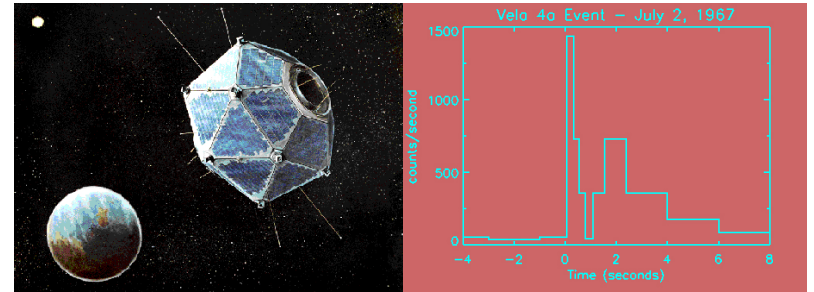
Observations

- 1967: the first GRB
Vela satellites
(first publication on 1973)



Observations

- **1967: the first GRB**
Vela satellites
(first publication on 1973)
- **1991: launch of Compton Gamma Ray Observatory**
Burst and Transient Experiment (BATSE)
2704 GRBs (until May 2000)
isotropic distribution (cosmological origin)

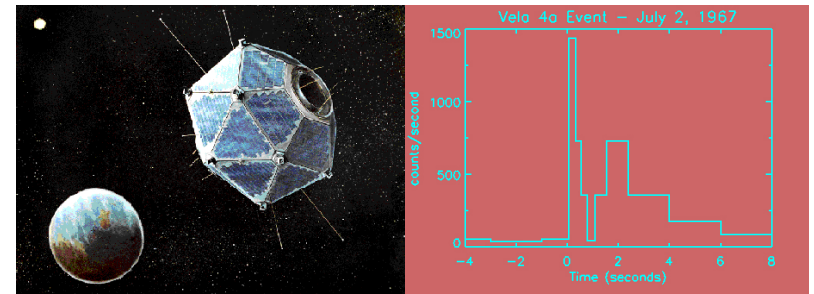


Observations

- 1967: the first GRB

Vela satellites

(first publication on 1973)



- 1991: launch of Compton Gamma Ray Observatory

Burst and Transient Experiment (BATSE)

2704 GRBs (until May 2000)

isotropic distribution (cosmological origin)



- 1997: Beppo (in honor of Giuseppe Occhialini) Satellite per Astronomia X

X-ray afterglow

arc-min accuracy positions

optical detection

GRB afterglow at longer wavelengths

identification of the host galaxy

measurement of redshift distances

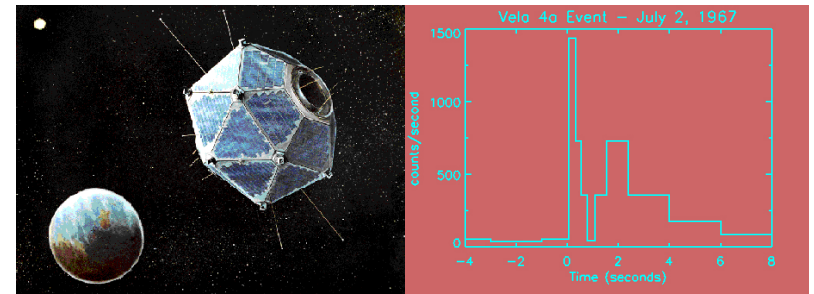


Observations

- 1967: the first GRB

Vela satellites

(first publication on 1973)



- 1991: launch of Compton Gamma Ray Observatory

Burst and Transient Experiment (BATSE)

2704 GRBs (until May 2000)

isotropic distribution (cosmological origin)



- 1997: Beppo (in honor of Giuseppe Occhialini) Satellite per Astronomia X

X-ray afterglow

arc-min accuracy positions

optical detection

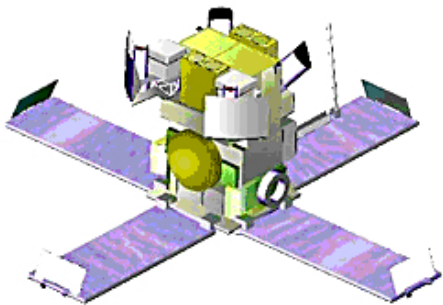
GRB afterglow at longer wavelengths

identification of the host galaxy

measurement of redshift distances



- High Energy Transient Explorer-2

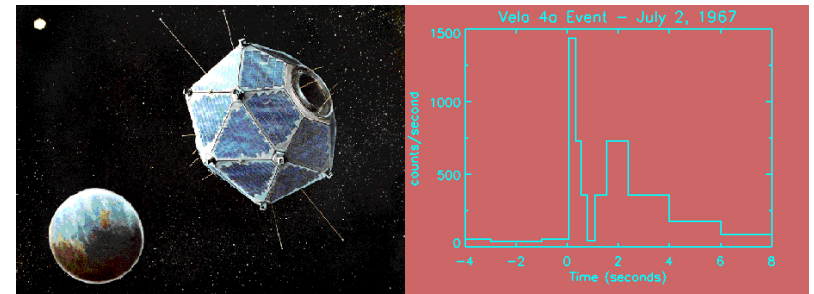


Observations

- 1967: the first GRB

Vela satellites

(first publication on 1973)

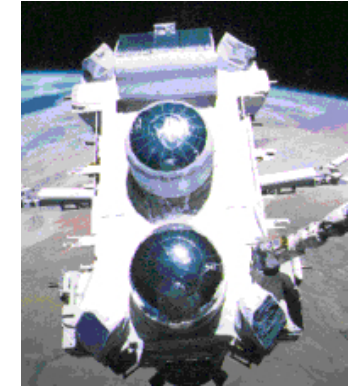


- 1991: launch of Compton Gamma Ray Observatory

Burst and Transient Experiment (BATSE)

2704 GRBs (until May 2000)

isotropic distribution (cosmological origin)



- 1997: Beppo (in honor of Giuseppe Occhialini) Satellite per Astronomia X

X-ray afterglow

arc-min accuracy positions

optical detection

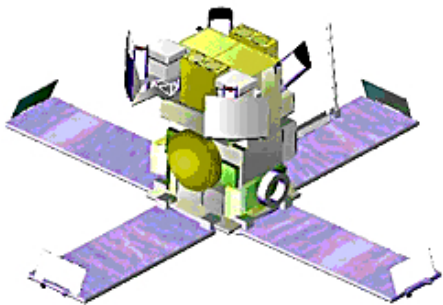
GRB afterglow at longer wavelengths

identification of the host galaxy

measurement of redshift distances



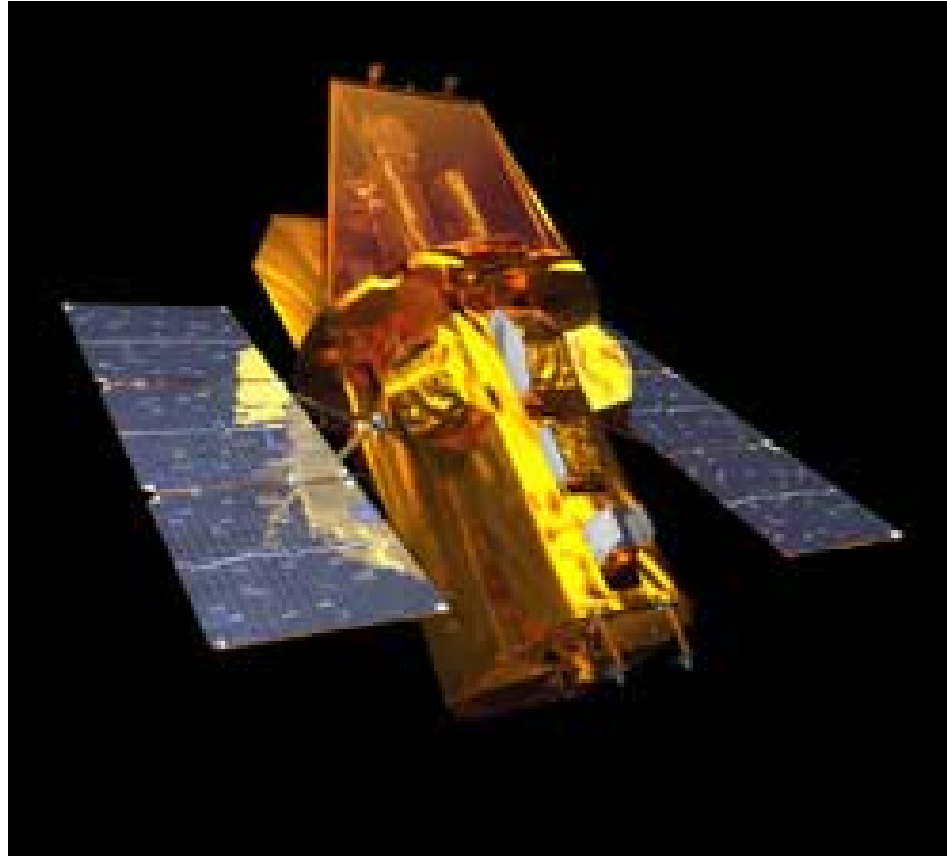
- High Energy Transient Explorer-2



- International Gamma-Ray Astrophysics Laboratory



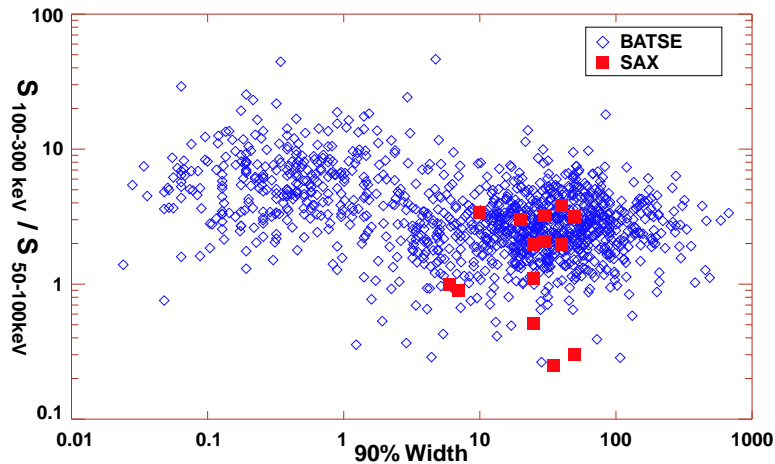
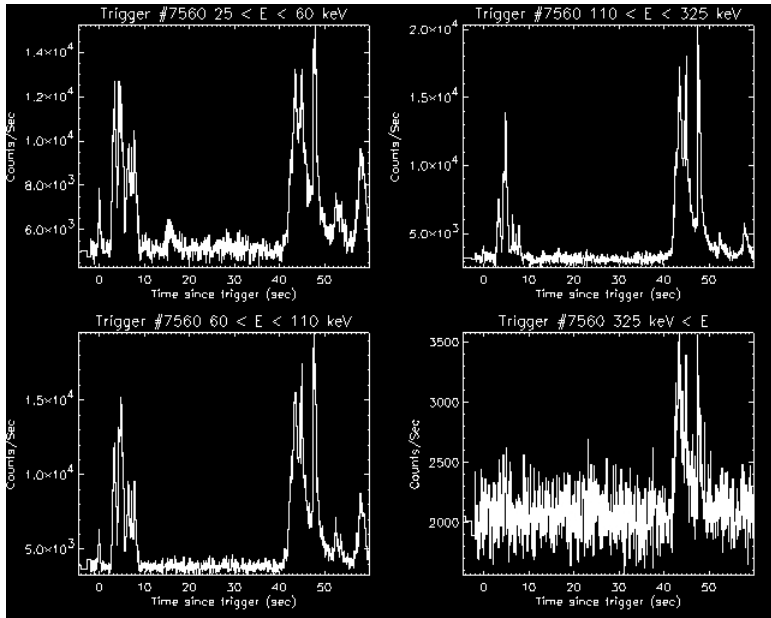
Swift



<http://swift.gsfc.nasa.gov>

Gamma-ray Burst Real-time Sky Map @ <http://grb.sonoma.edu/>

GRB prompt emission



(from Djorgovski et al. 2001)

- Fluence $F_\gamma = 10^{-8} - 10^{-3} \text{ ergs/cm}^2$
energy

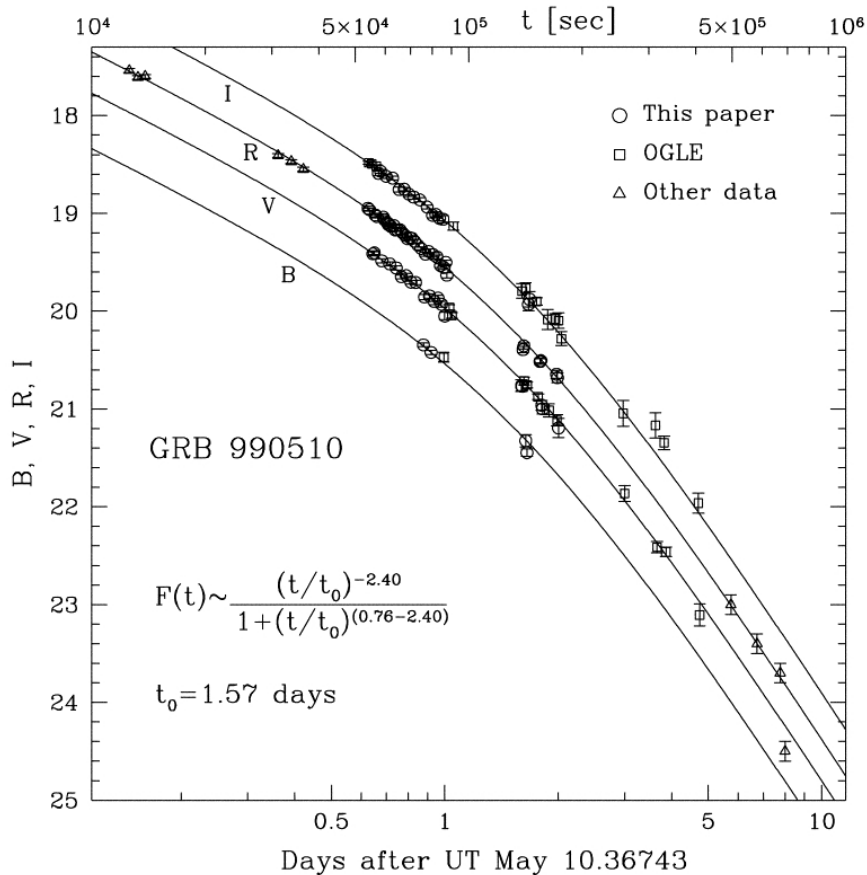
$$E_\gamma = 10^{53} \left(\frac{D}{3 \text{ Gpc}} \right)^2 \left(\frac{F_\gamma}{10^{-4} \frac{\text{ergs}}{\text{cm}^2}} \right) \left(\frac{\Delta\omega}{4\pi} \right) \text{ ergs}$$

collimation $\left\{ \begin{array}{l} \text{reduces } E_\gamma \\ \text{increases the rate of events} \end{array} \right.$

- non-thermal spectrum
- Duration $\Delta t = 10^{-3} - 10^3 \text{ s}$
long bursts $> 2 \text{ s}$, short bursts $< 2 \text{ s}$
- Variability $\delta t = \Delta t / N$, $N = 1 - 1000$
compact source $R < c \delta t \sim 1000 \text{ km}$
not a single explosion
huge optical depth for $\gamma\gamma \rightarrow e^+e^-$
compactness problem: how the photons escape?

relativistic motion $\left\{ \begin{array}{l} R < \gamma^2 c \delta t \\ \text{blueshifted photon energy} \\ \text{beaming} \\ \text{optically thin} \end{array} \right.$
 $\gamma \gtrsim 100$

Afterglow



(from Stanek et al. 1999)

- from X-rays to radio
- fading – broken power law
 panchromatic break $F_\nu \propto \begin{cases} t^{-a_1}, & t < t_0 \\ t^{-a_2}, & t > t_0 \end{cases}$
- non-thermal spectrum
 (synchrotron + inverse Compton
 with power law electron energy distribution)

The internal–external shocks model

mass outflow (pancake)

N shells (moving with different $\gamma \gg 1$)

Frozen pulse

(if ℓ the path's arclength,

$s \equiv ct - \ell = \text{const}$ for each shell,

$\delta s = \text{const}$ for two shells)

internal shocks

(a few tens of kinetic energy \rightarrow **GRB**)

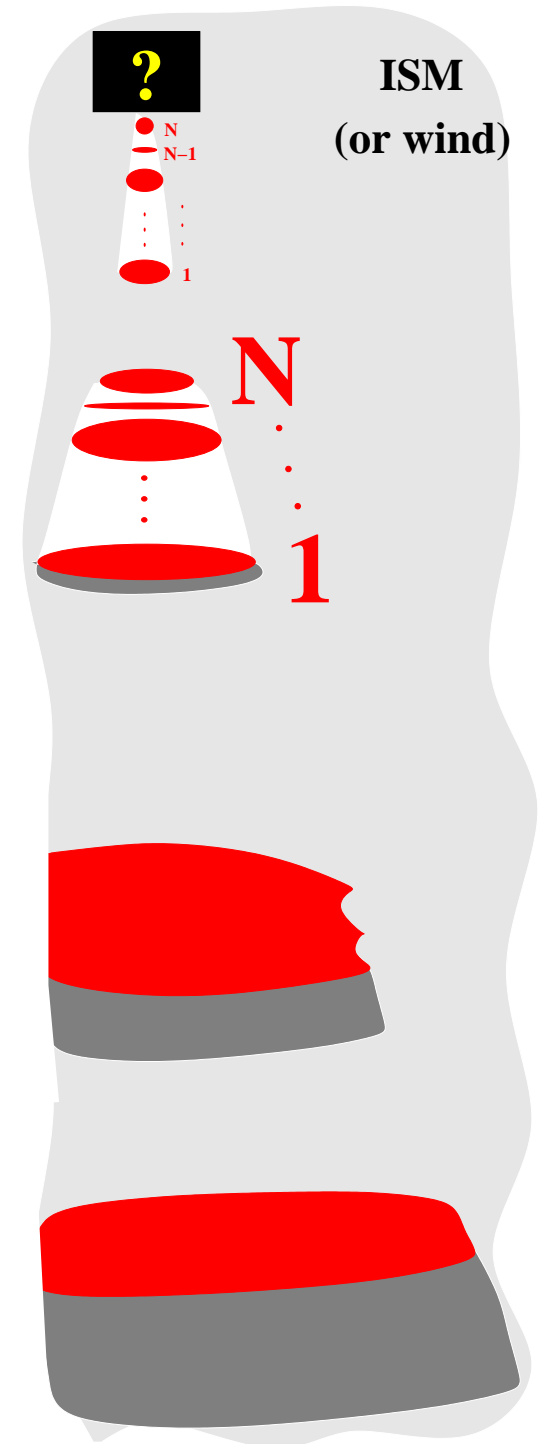
external shock

interaction with ISM (or wind)

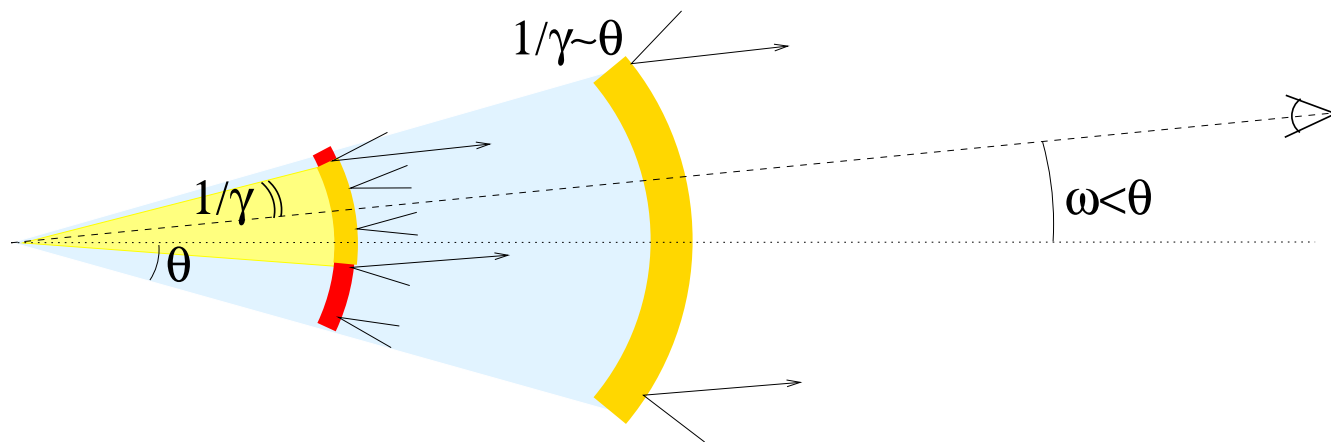
(when the flow accumulates $M_{ISM} = M/\gamma$)

As γ decreases with time, kinetic energy \rightarrow X-rays ... radio

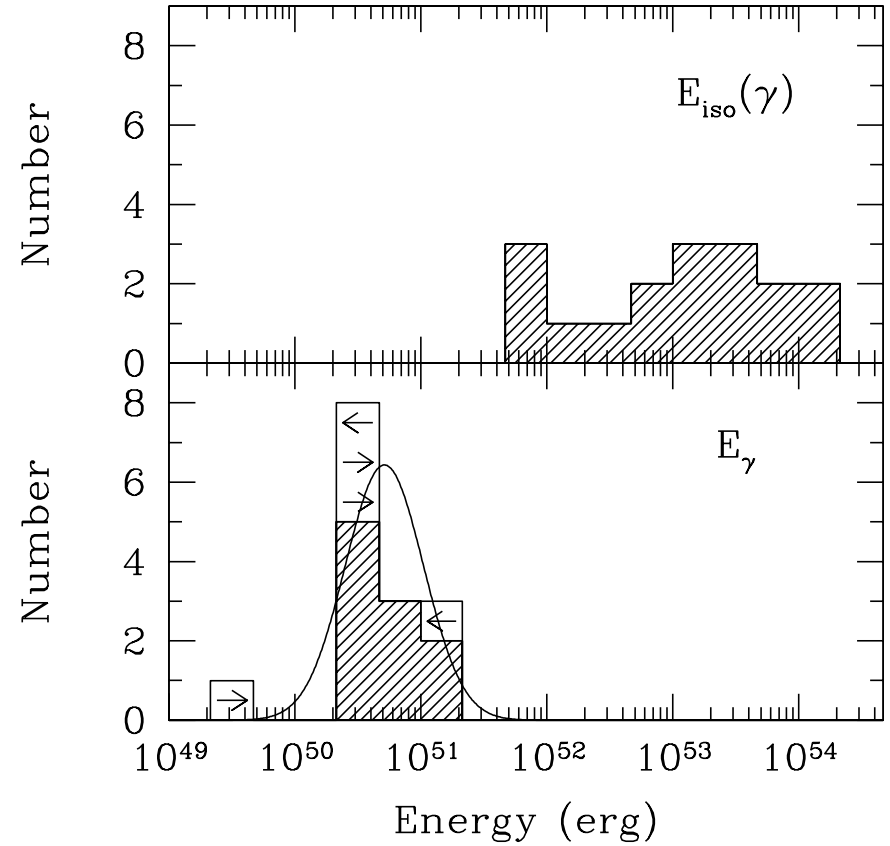
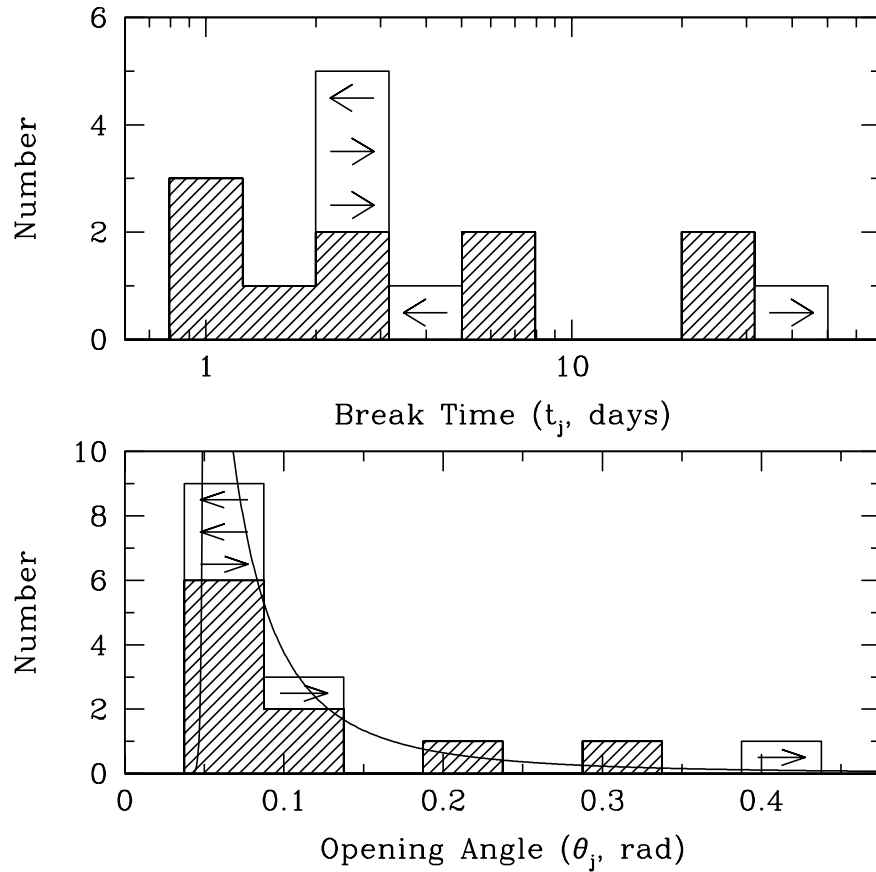
\rightarrow **Afterglow**



Beaming – Collimation



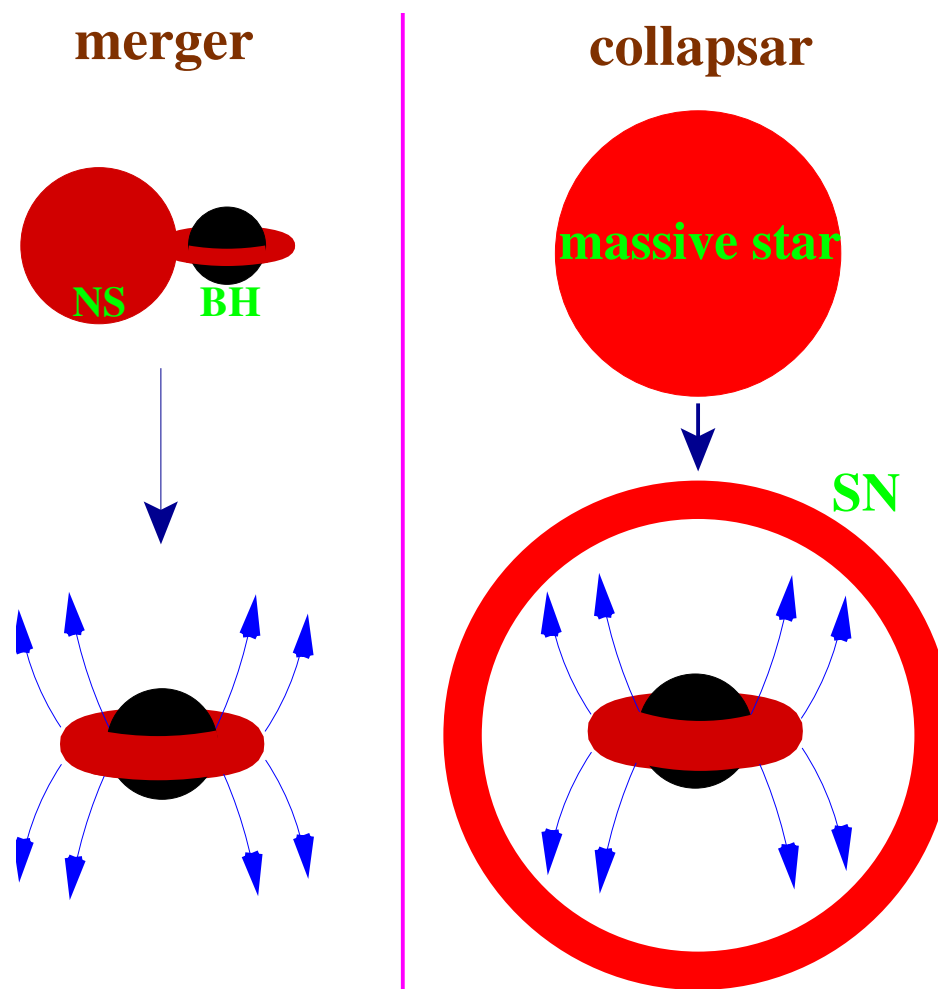
- During the afterglow γ decreases
When $1/\gamma > \vartheta$ the $F(t)$ decreases faster
The broken power-law justifies collimation
- orphan afterglows ?
(for $\omega > \vartheta$)



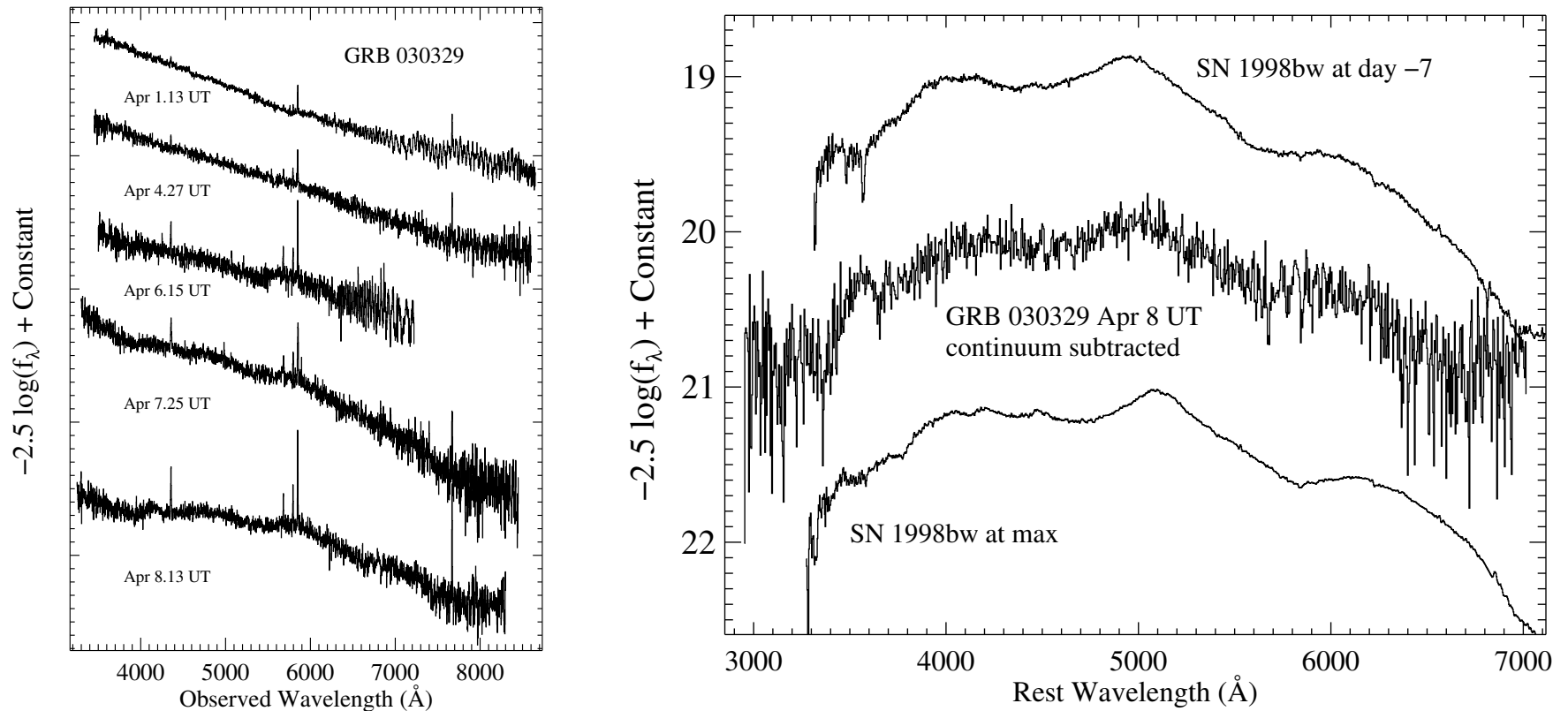
- afterglow fits \rightarrow
 - opening half-angle $\vartheta = 1^\circ - 10^\circ$
 - energy $E_\gamma = 10^{50} - 10^{51}$ ergs (Frail et al. 2001)
 - $E_{\text{afterglow}} = 10^{50} - 10^{51}$ ergs (Panaitescu & Kumar 2002)

Imagine a Progenitor ...

- **acceleration** and **collimation** of matter ejecta
- $E \sim 1\%$ of the binding energy of a solar-mass compact object
- small $\delta t \rightarrow$ compact object
- highly relativistic \rightarrow compact object
- two time scales ($\delta t, \Delta t$) + energetics suggest accretion



The supernova connection



Left: Spectrum evolution, from 2.64 to 9.64 days after the burst.

Right: Spectrum of April 8 with the smoothed spectrum of April 1 scaled and subtracted. (From Stanek et al. 2003)

The SN exploded within a few days of the GRB (Hjorth et al. Nature 2003).

The BH – debris-disk system

- **Energy reservoirs:**

- ① binding energy of the orbiting debris
- ② spin energy of the newly formed BH

The BH – debris-disk system

- **Energy reservoirs:**

- ① binding energy of the orbiting debris
- ② spin energy of the newly formed BH

- **Energy extraction mechanisms:**

- ☞ viscous dissipation \Rightarrow thermal energy $\Rightarrow \nu\bar{\nu} \rightarrow e^+e^- \Rightarrow e^\pm/\text{photon}/\text{baryon}$ **fireball**
 - unlikely that the disk is optically thin to neutrinos (Di Matteo, Perna, & Narayan 2002)
 - strong photospheric emission would have been detectable (Daigne & Mochkovitch 2002)
 - difficult to explain the collimation
 - highly super-Eddington luminosity usually implies high baryonic mass \rightarrow small γ

The BH – debris-disk system

• Energy reservoirs:

- ① binding energy of the orbiting debris
- ② spin energy of the newly formed BH

• Energy extraction mechanisms:

- ☞ viscous dissipation \Rightarrow thermal energy $\Rightarrow \nu\bar{\nu} \rightarrow e^+e^- \Rightarrow e^\pm/\text{photon}/\text{baryon}$ **fireball**
 - unlikely that the disk is optically thin to neutrinos (Di Matteo, Perna, & Narayan 2002)
 - strong photospheric emission would have been detectable (Daigne & Mochkovitch 2002)
 - difficult to explain the collimation
 - highly super-Eddington luminosity usually implies high baryonic mass \rightarrow small γ
- ☞ dissipation of magnetic fields
 - generated by the differential rotation in the torus $\Rightarrow e^\pm/\text{photon}/\text{baryon}$ “magnetic” **fireball**
 - collimation
 - strong photospheric emission \Rightarrow detectable thermal emission

➔ MHD extraction (**Poynting** jet)

- $\mathcal{E} = \frac{c}{4\pi} \underbrace{\frac{\varpi\Omega}{c}}_E B_p B_\phi \times \text{area} \times \text{duration} \Rightarrow$

$$\frac{B_p B_\phi}{(2 \times 10^{14} \text{G})^2} = \left[\frac{\mathcal{E}}{5 \times 10^{51} \text{ergs}} \right] \left[\frac{\text{area}}{4\pi \times 10^{12} \text{cm}^2} \right]^{-1} \left[\frac{\varpi\Omega}{10^{10} \text{cm s}^{-1}} \right]^{-1} \left[\frac{\text{duration}}{10\text{s}} \right]^{-1}$$

- from the BH: $B_p \gtrsim 10^{15} \text{G}$ (small B_ϕ , small area)

- from the disk: smaller magnetic field required $\sim 10^{14} \text{G}$

- If initially $B_p/B_\phi > 1$, a **trans-Alfvénic** outflow is produced.

- If initially $B_p/B_\phi < 1$, the outflow is **super-Alfvénic** from the start.

- Is it possible to “use” this energy and accelerate the matter ejecta?

Ideal Magneto-Hydro-Dynamics

in collaboration with Arie König (U of Chicago)

- Outflowing matter:
 - baryons (rest density ρ_0)
 - ambient electrons (neutralize the protons)
 - e^\pm pairs (Maxwellian distribution)
- photons (blackbody distribution)
- large scale electromagnetic field \mathbf{E} , \mathbf{B}

$\tau \gg 1$ ensure local thermodynamic equilibrium

$$\left. \begin{array}{l} \text{charge density } \frac{J^0}{c} \ll \frac{\rho_0}{m_p} e \\ \text{current density } J \ll \frac{\rho_0}{m_p} e c \end{array} \right\} \text{one fluid approximation}$$

\mathbf{V} bulk velocity

P = total pressure (matter + radiation)

ξc^2 = specific enthalpy (matter + radiation)

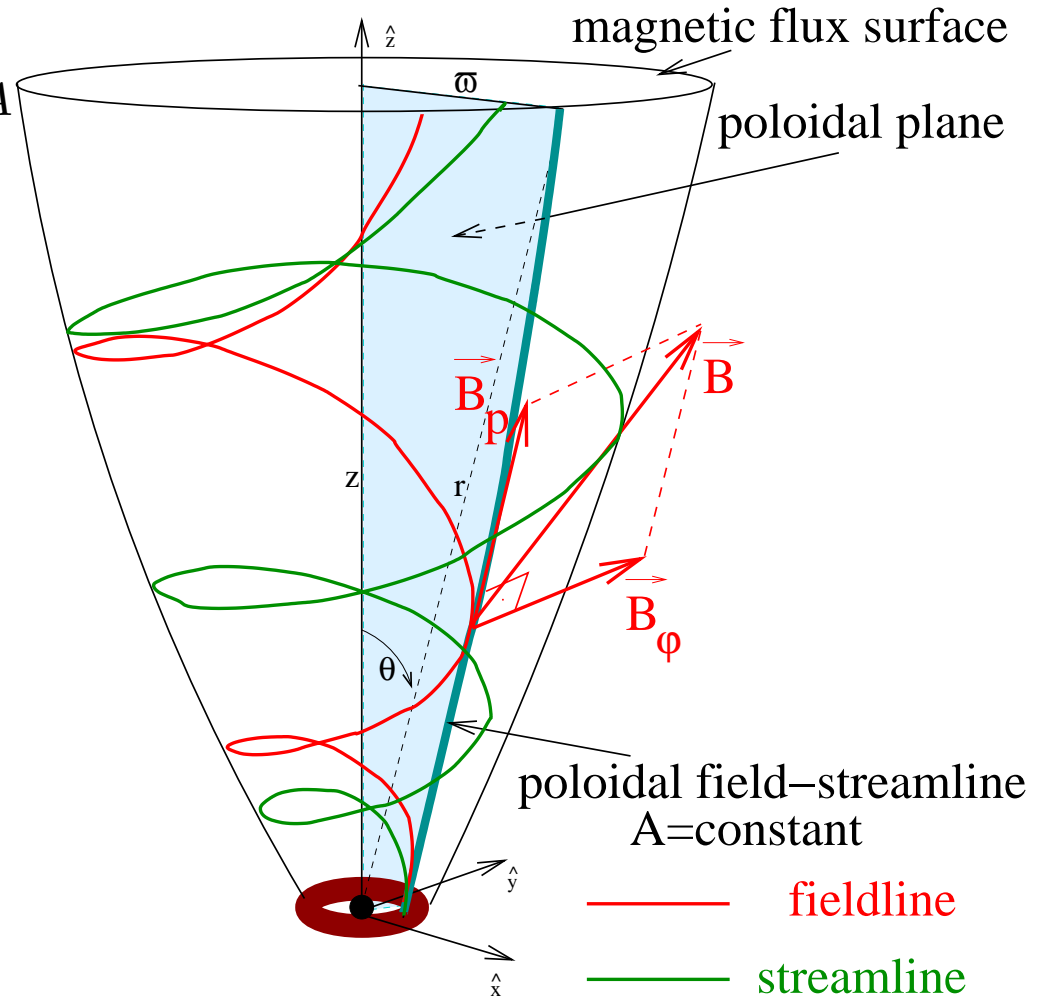
Assumptions

- ① axisymmetry
- ② highly relativistic poloidal motion
- ③ quasi-steady poloidal magnetic field $\Leftrightarrow E_\phi = 0 \Leftrightarrow \mathbf{B}_p \parallel \mathbf{V}_p$

Introduce the magnetic flux function A

$$\mathbf{B} = \mathbf{B}_p + \mathbf{B}_\phi, \quad \mathbf{B}_p = \nabla \times \left(A \frac{\hat{\phi}}{\varpi} \right)$$

$$\text{Faraday + Ohm} \rightarrow \mathbf{V}_p \parallel \mathbf{B}_p$$



The frozen-pulse approximation

- The arclength along a poloidal fieldline

$$\ell = \int_{\frac{s}{c}}^t V_p dt \approx ct - s \Rightarrow s = ct - \ell$$

- s is constant for each ejected shell. Moreover, the distance between two different shells $\ell_2 - \ell_1 = s_1 - s_2$ remains the same (even if they move with $\gamma_1 \neq \gamma_2$).

- **Eliminating t in terms of s** , we show that all terms with $\partial/\partial s$ are $\mathcal{O}(1/\gamma) \times$ remaining terms (generalizing the HD case examined by Piran, Shemi, & Narayan 1993). Thus **we may examine the motion of each shell using steady-state equations.**

$$\left(\text{e.g., } \frac{d}{dt} = (c - V_p) \frac{\partial}{\partial s} + \mathbf{V} \cdot \nabla_s \approx \mathbf{V} \cdot \nabla_s \right)$$

(also $E = |\mathbf{B} \times \mathbf{V}/c| \approx |\mathbf{B} \times \mathbf{V}_p/c| \approx |B_\phi|$)

Integration

The full set of ideal MHD equations can be partially integrated to yield five fieldline constants (**functions of A and $s = ct - \ell$**):

- ① the mass-to-magnetic flux ratio
- ② the field angular velocity
- ③ the specific angular momentum
- ④ the total energy-to-mass flux ratio μc^2
- ⑤ the adiabat $P/\rho_0^{4/3}$

Two integrals remain to be performed, involving the **Bernoulli and transfield force-balance** equations.

Known solutions of the ideal MHD equations

Michel's solution gives $\gamma_\infty = \mu^{1/3}$ and $\sigma_\infty = \mu^{2/3} \gg 1$
($\mu c^2 = \frac{\text{total energy flux}}{\text{mass flux}}$; μ is the maximum possible γ).

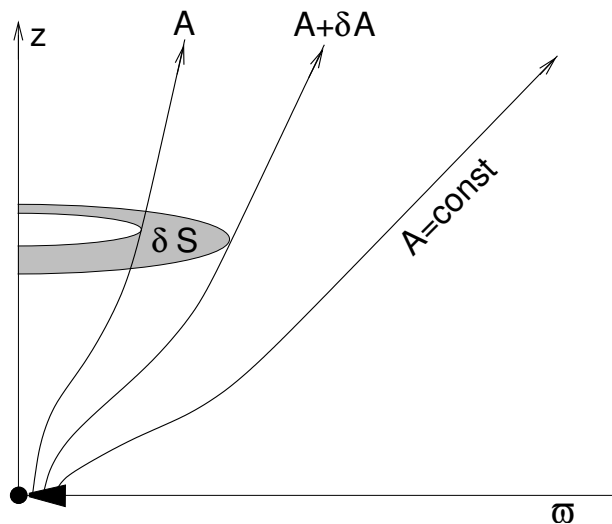
BUT, it does not satisfy the transfield equation.

Known solutions of the ideal MHD equations

Michel's solution gives $\gamma_\infty = \mu^{1/3}$ and $\sigma_\infty = \mu^{2/3} \gg 1$
 ($\mu c^2 = \frac{\text{total energy flux}}{\text{mass flux}}$; μ is the maximum possible γ).

BUT, it does not satisfy the transfield equation.

Necessary to solve the transfield because the line shape controls the acceleration:



Poynting-to-mass flux ratio $\propto \varpi |B_\phi| \rightarrow$
 $\gamma \uparrow$ when $\varpi |B_\phi| \downarrow$
 $E = |\mathbf{V}/c \times \mathbf{B}| \approx |B_\phi|$, $E = (\varpi\Omega/c)B_p$
 So, $\varpi |B_\phi| \propto \varpi^2 B_p = (\varpi^2/\delta S)\delta A$
 ($A =$ magnetic flux function).

Trying to solve the transfield

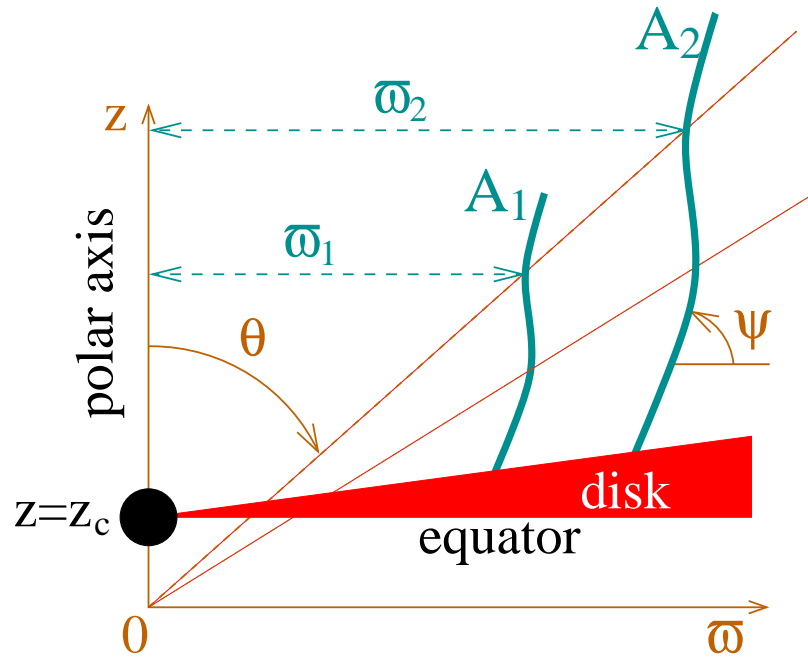
Bernoulli is algebraic

The transfield is a 2nd order PDE of the form

$$a \frac{\partial^2 A}{\partial \varpi^2} + 2b \frac{\partial^2 A}{\partial \varpi \partial z} + c \frac{\partial^2 A}{\partial z^2} = d, \quad a, b, c, d = \text{functions of } \frac{\partial A}{\partial \varpi}, \frac{\partial A}{\partial z}, A, \varpi$$

- mixed type → extremely difficult numerical work (no solution at present)
- easier to solve numerically the time-dependent flow (only a few rotational periods)
- mixed (Bogovalov)
- analytical solutions: Only one exact solution known: the steady-state, cold, r self-similar model found by Li, Chiueh, & Begelman (1992) and Contopoulos (1994).
Generalization for non-steady GRB outflows, including radiation and thermal effects.

r self-similarity



self-similar ansatz $r = \mathcal{F}_1(A) \mathcal{F}_2(\theta)$

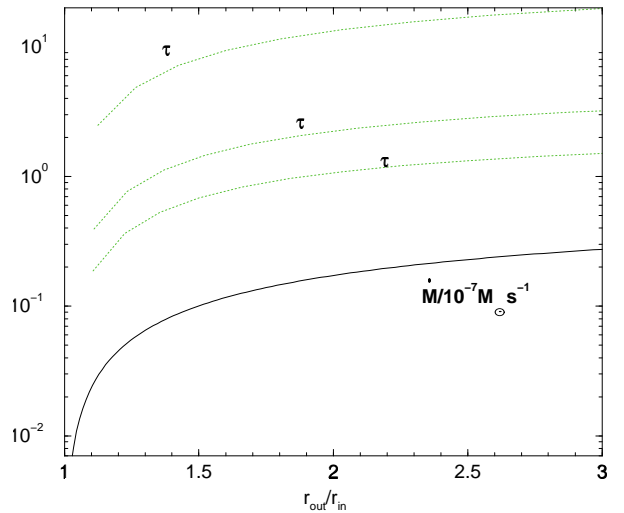
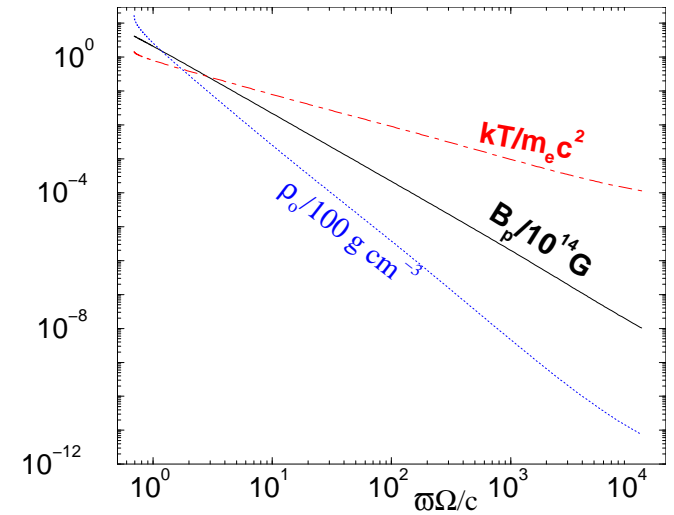
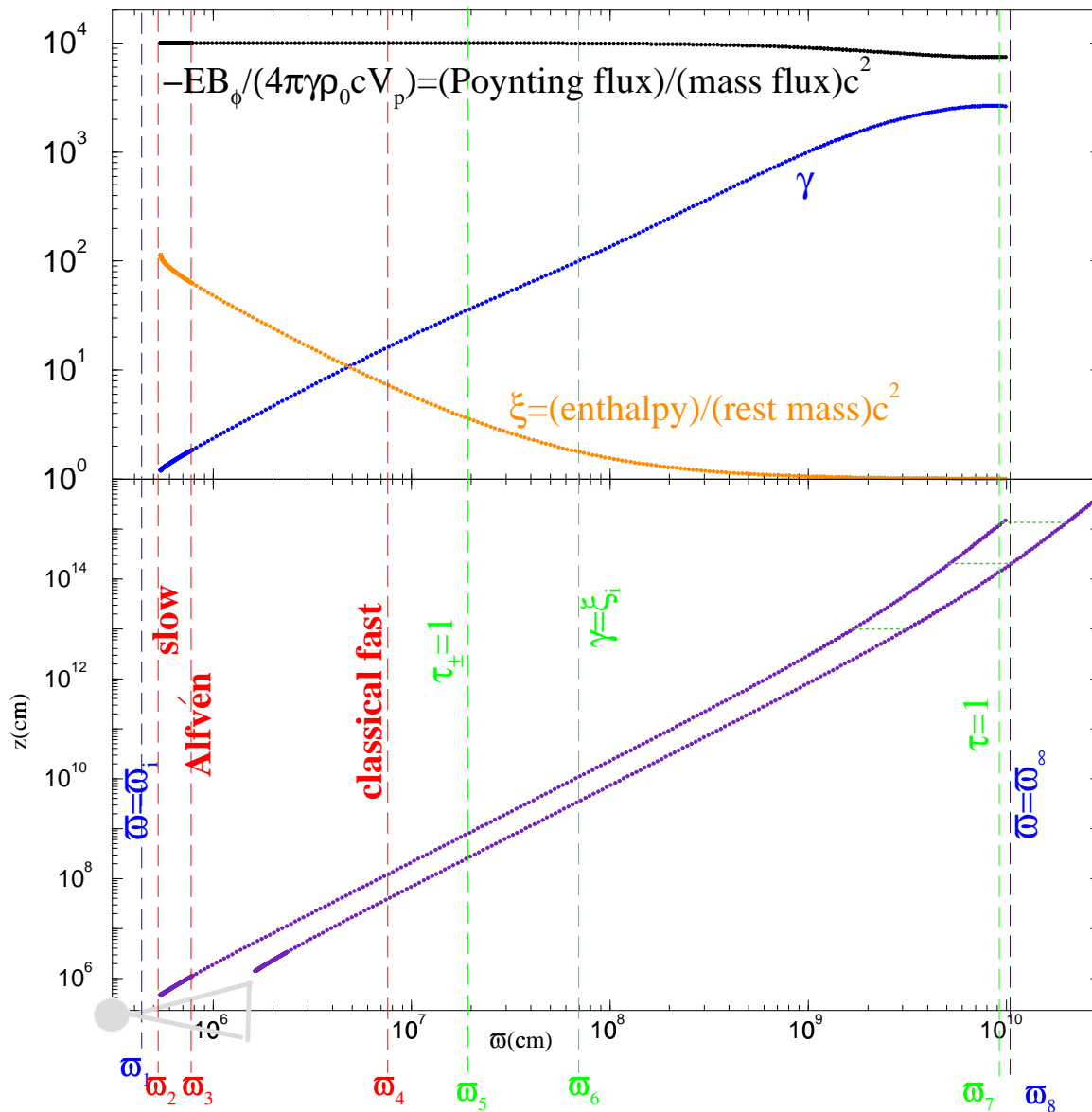
For points on the same cone $\theta = const$,

$$\frac{\omega_1}{\omega_2} = \frac{r_1}{r_2} = \frac{\mathcal{F}_1(A_1)}{\mathcal{F}_1(A_2)}.$$

$$\text{ODEs} \left\{ \begin{array}{l} \psi = \psi(x, M, \theta), \text{ (Bernoulli)} \\ \frac{dx}{d\theta} = \mathcal{N}_0(x, M, \psi, \theta), \text{ (definition of } \psi) \\ \frac{dM}{d\theta} = \frac{\mathcal{N}(x, M, \psi, \theta)}{\mathcal{D}(x, M, \psi, \theta)}, \text{ (transfield)} \end{array} \right\} \begin{array}{l} \mathcal{D} = 0 : \text{ singular points} \\ \text{(Alfvén, modified slow - fast)} \end{array}$$

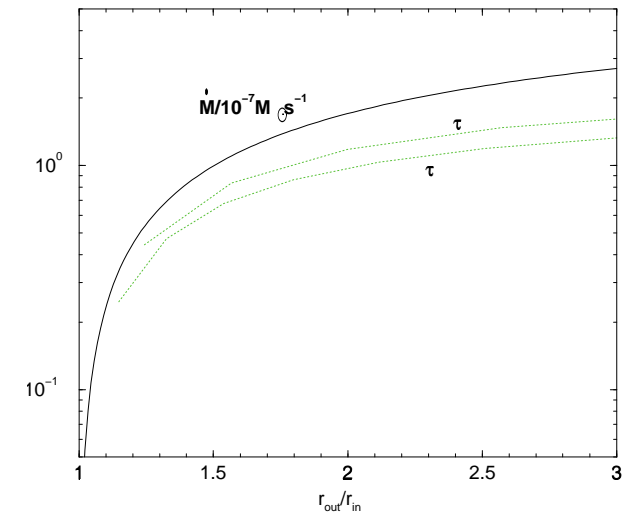
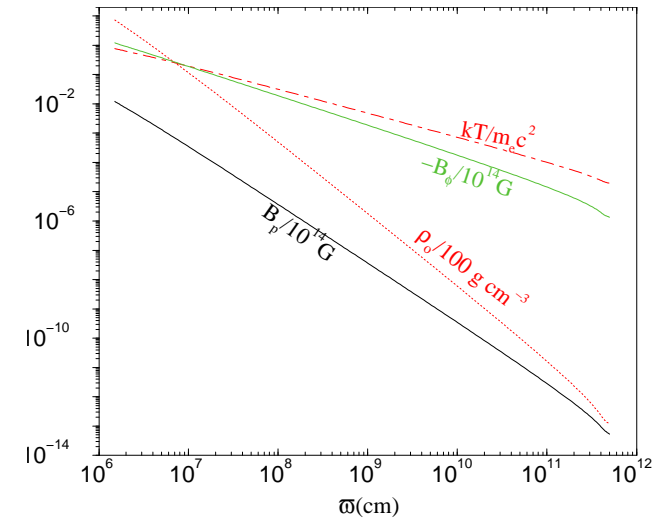
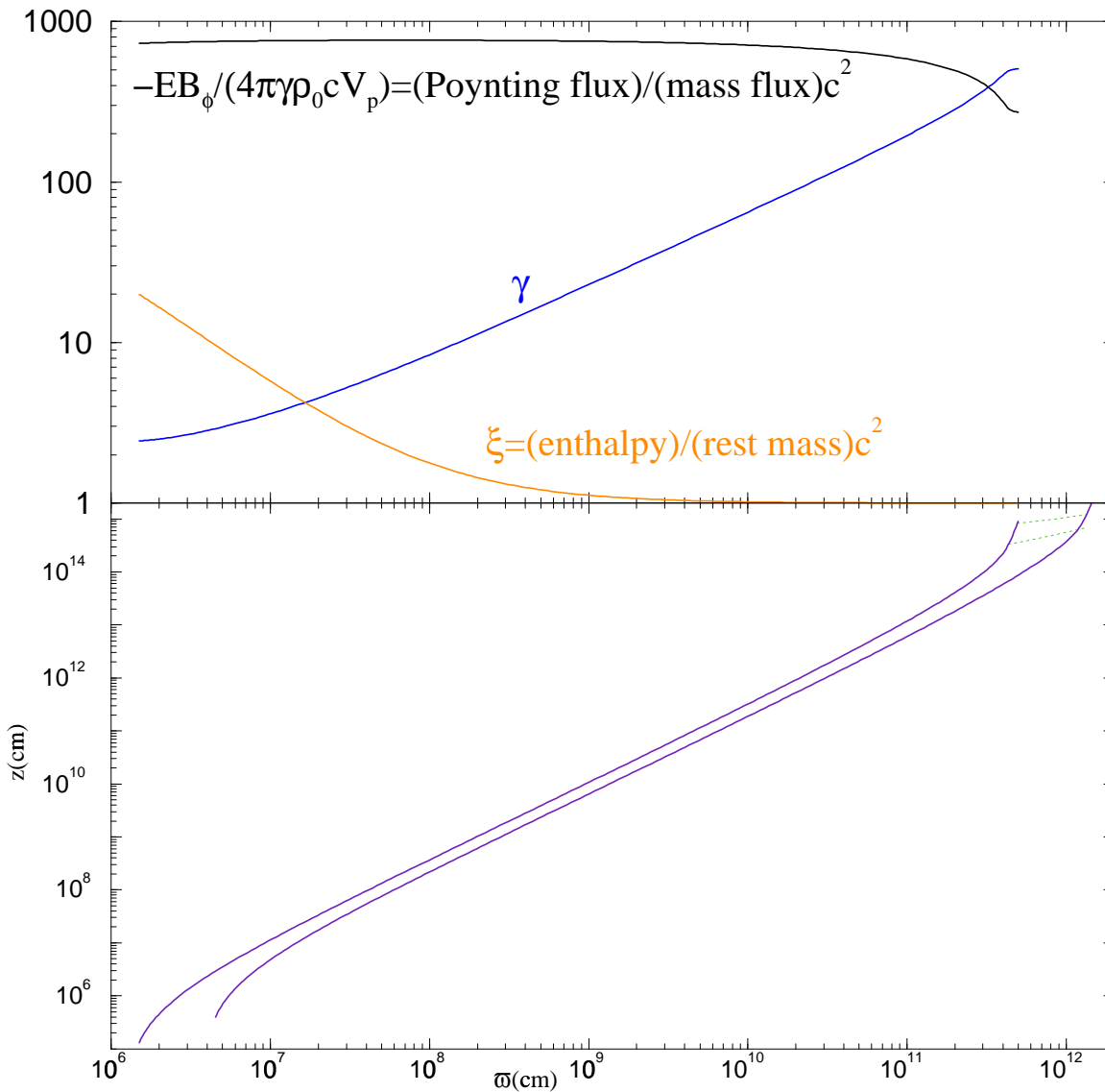
(start the integration from a cone $\theta = \theta_i$ and give the boundary conditions $B_\theta = -C_1 r^{F-2}$, $B_\phi = -C_2 r^{F-2}$, $V_r/c = C_3$, $V_\theta/c = -C_4$, $V_\phi/c = C_5$, $\rho_0 = C_6 r^{2(F-2)}$, and $P = C_7 r^{2(F-2)}$, where F = parameter).

Trans-Alfvénic Jets (NV & Königl 2001, 2003a)



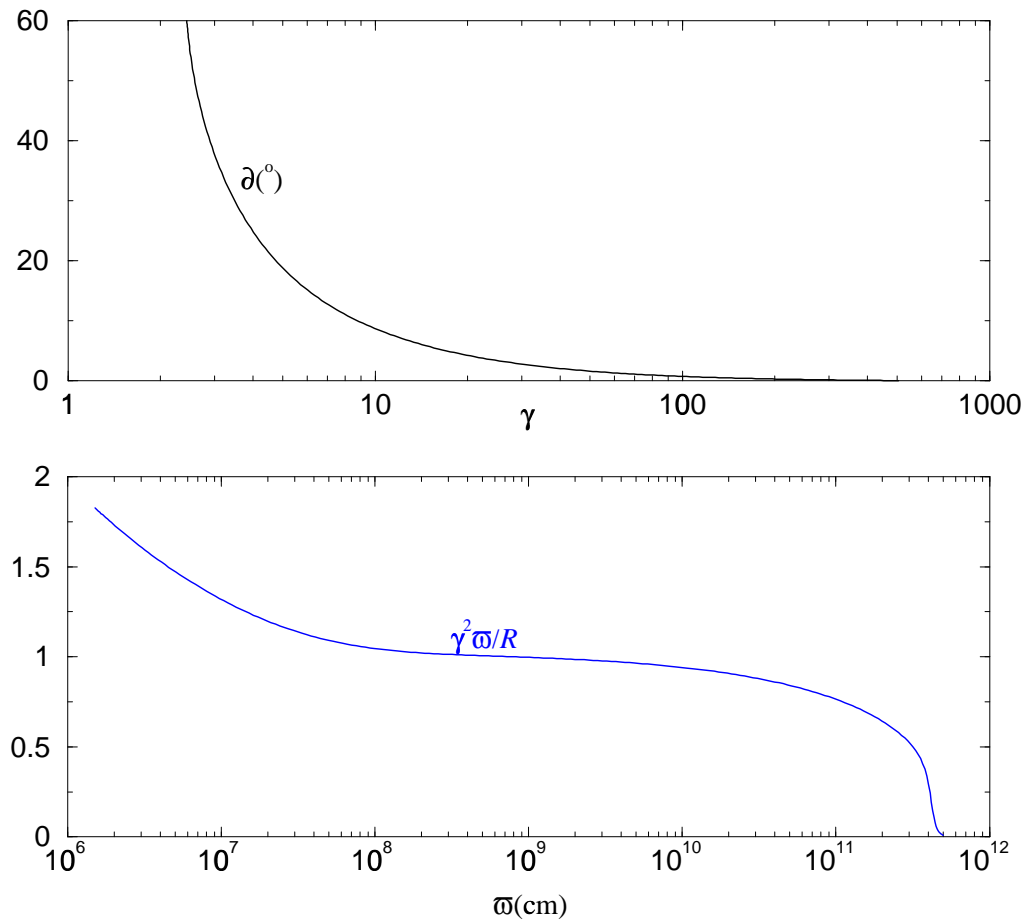
- $\omega_1 < \omega < \omega_6$: **Thermal acceleration** - force free magnetic field ($\gamma \propto \omega$, $\rho_0 \propto \omega^{-3}$, $T \propto \omega^{-1}$, $\omega B_\phi = const$, parabolic shape of fieldlines: $z \propto \omega^2$)
- $\omega_6 < \omega < \omega_8$: **Magnetic acceleration** ($\gamma \propto \omega$, $\rho_0 \propto \omega^{-3}$)
- $\omega = \omega_8$: **cylindrical regime** - equipartition $\gamma_\infty \approx (-EB_\phi/4\pi\gamma\rho_0 V_p)_\infty$

Super-Alfvénic Jets (NV & Königl 2003b)



- **Thermal acceleration** ($\gamma \propto r^{0.44}$, $\rho_0 \propto r^{-2.4}$, $T \propto r^{-0.8}$, $B_\phi \propto r^{-1}$, $z \propto r^{1.5}$)
- **Magnetic acceleration** ($\gamma \propto r^{0.44}$, $\rho_0 \propto r^{-2.4}$)
- **cylindrical regime - equipartition** $\gamma_\infty \approx (-EB_\phi/4\pi\gamma\rho_0V_p)_\infty$

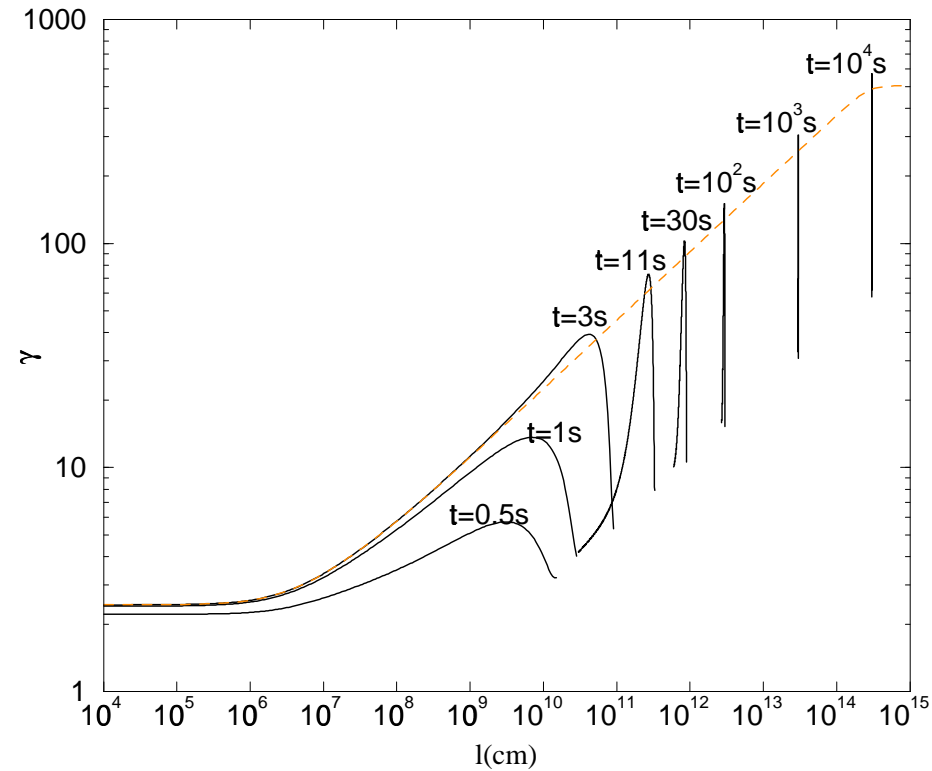
Collimation



- ★ At $\varpi = 10^8$ cm – where $\gamma = 10$ – the opening half-angle is already $\vartheta = 10^\circ$
- ★ For $\varpi > 10^8$ cm, collimation continues slowly ($\mathcal{R} \sim \gamma^2 \varpi$)

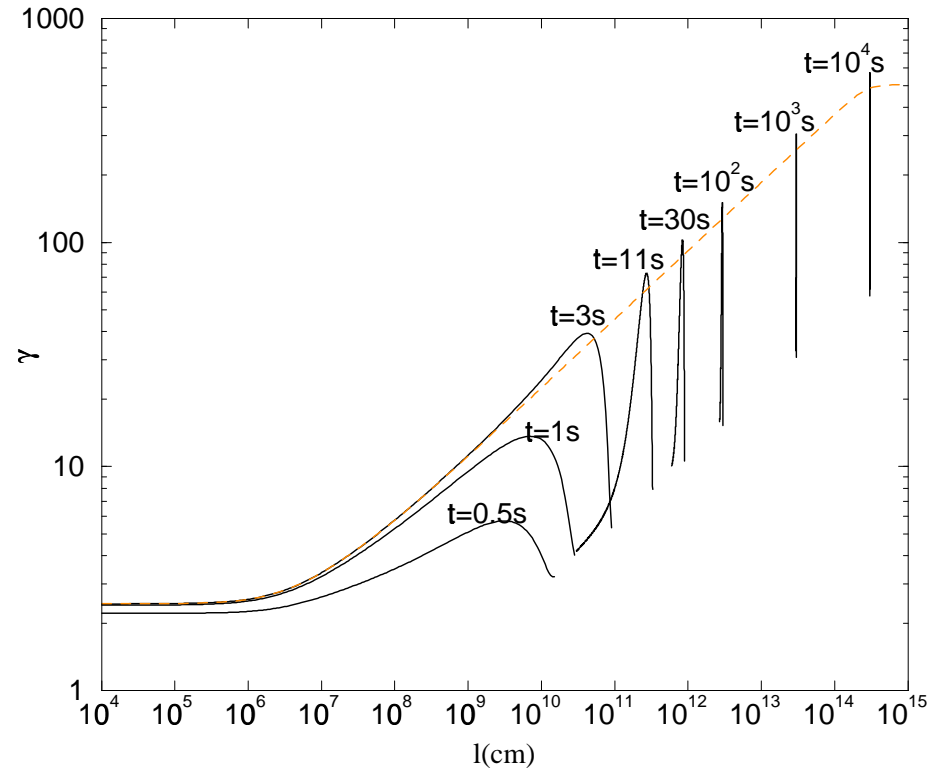
Time-Dependent Effects

★ recovering the time-dependence:



Time-Dependent Effects

★ recovering the time-dependence:



★ internal shocks:

The distance between two neighboring shells $s_1, s_2 = s_1 + \delta s$

$$\delta \ell = \delta \left(\int_{\frac{s}{c}}^t V_p dt \right) = -\delta s - \delta \left(\int_{\frac{s}{c}}^t (c - V_p) dt \right) \approx -\delta s - \int_0^t \delta \left(\frac{c}{2\gamma^2} \right) dt$$

Different $V_p \Rightarrow$ collision (at $ct \approx \gamma^2 \delta s$ – inside the cylindrical regime)

The baryon loading problem

- Proton mass in jet: $M_{\text{proton}} = 3 \times 10^{-6} (\mathcal{E}/10^{51} \text{ergs}) (\gamma_{\infty}/200)^{-1} M_{\odot}$.
- The disk would be $\sim 10^4$ times more massive even if 10% of its gravitational potential energy could be converted into outflow kinetic energy (baryon loading problem).

A possible resolution (Fuller et al. 2000):

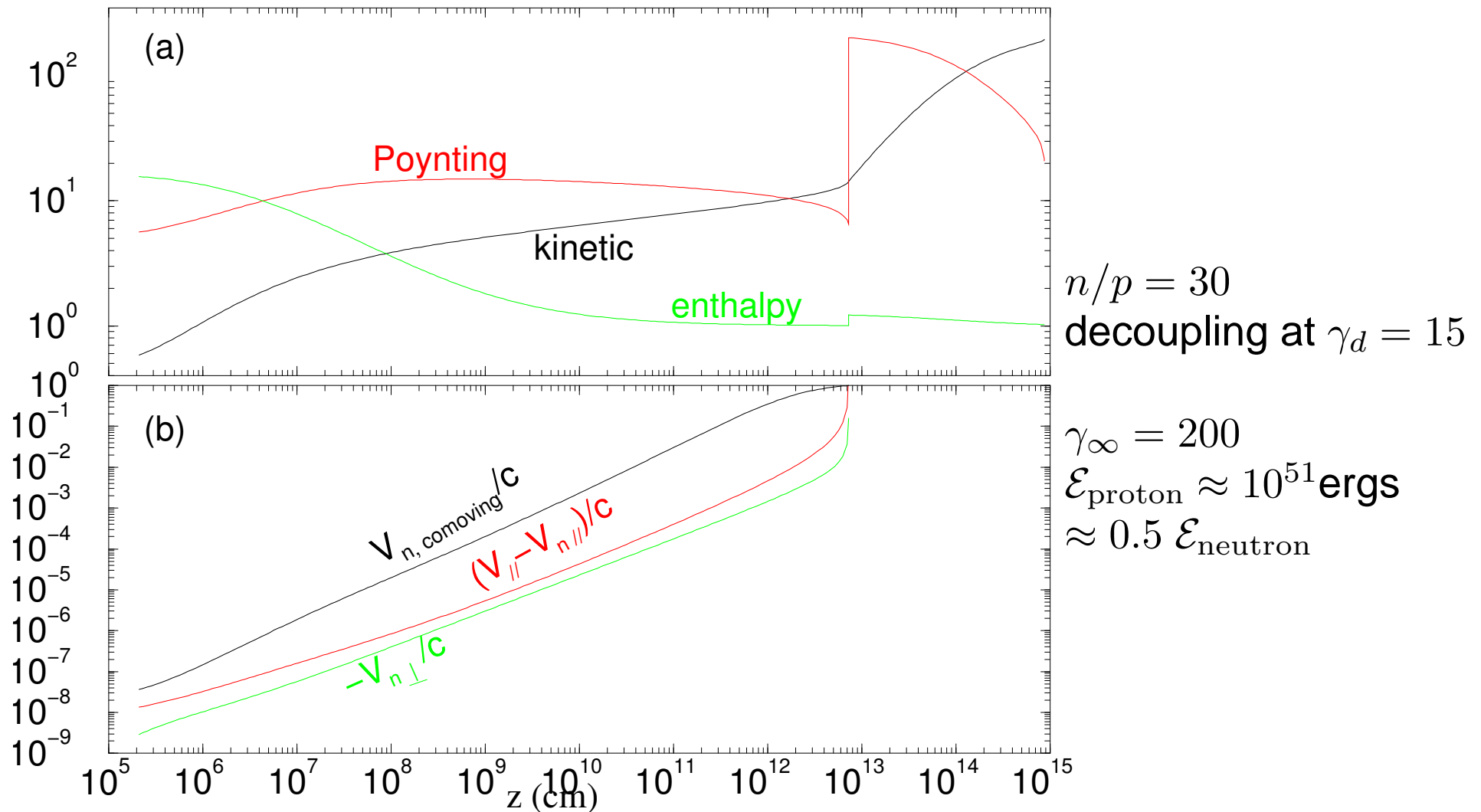
- If the source is neutron-rich, then the neutrons could decouple from the flow before the protons attain their terminal Lorentz factor.
- Disk-fed GRB outflows are expected to be neutron-rich, with n/p as high as $\sim 20 - 30$ (Pruet et al. 2003; Beloborodov 2003; Vlahakis et al. 2003).

However, it turns out that the decoupling Lorentz factor γ_d in a thermally driven, purely hydrodynamic outflow is of the order of the inferred value of γ_{∞} (e.g., Derishev et al. 1999; Beloborodov 2003), which has so far limited the practical implications of the Fuller et al. (2000) proposal.

Neutron-rich hydromagnetic flows

(Vlahakis, Peng, & Königl 2003 ApJL)

- Part of the thermal energy could be converted to electromagnetic (with the remainder transferred to baryon kinetic).
- The Lorentz factor increases with lower rate compared to the hydrodynamic case. This makes it possible to attain $\gamma_d \ll \gamma_\infty$, as it is shown in the following solution.
- The energy deposited into the Poynting flux is returned to the matter beyond the decoupling point.
- Pre-decoupling phase:
 - The momentum equation for the whole system (protons/neutrons/ e^\pm /photons/electromagnetic field) yields the flow velocity.
 - The momentum equation for the neutrons alone yields the neutron-proton collisional drag-force, and the drift velocity.
 - When $V_{\text{proton}} - V_{\text{neutron}} \sim c$ the neutrons decouple.
- Post-decoupling phase:
 - We solve for the protons alone (+ electromagnetic field).



(a) The three components of the total energy flux, normalized by the mass flux $\times c^2$.

(b) Proton–neutron drift velocity.

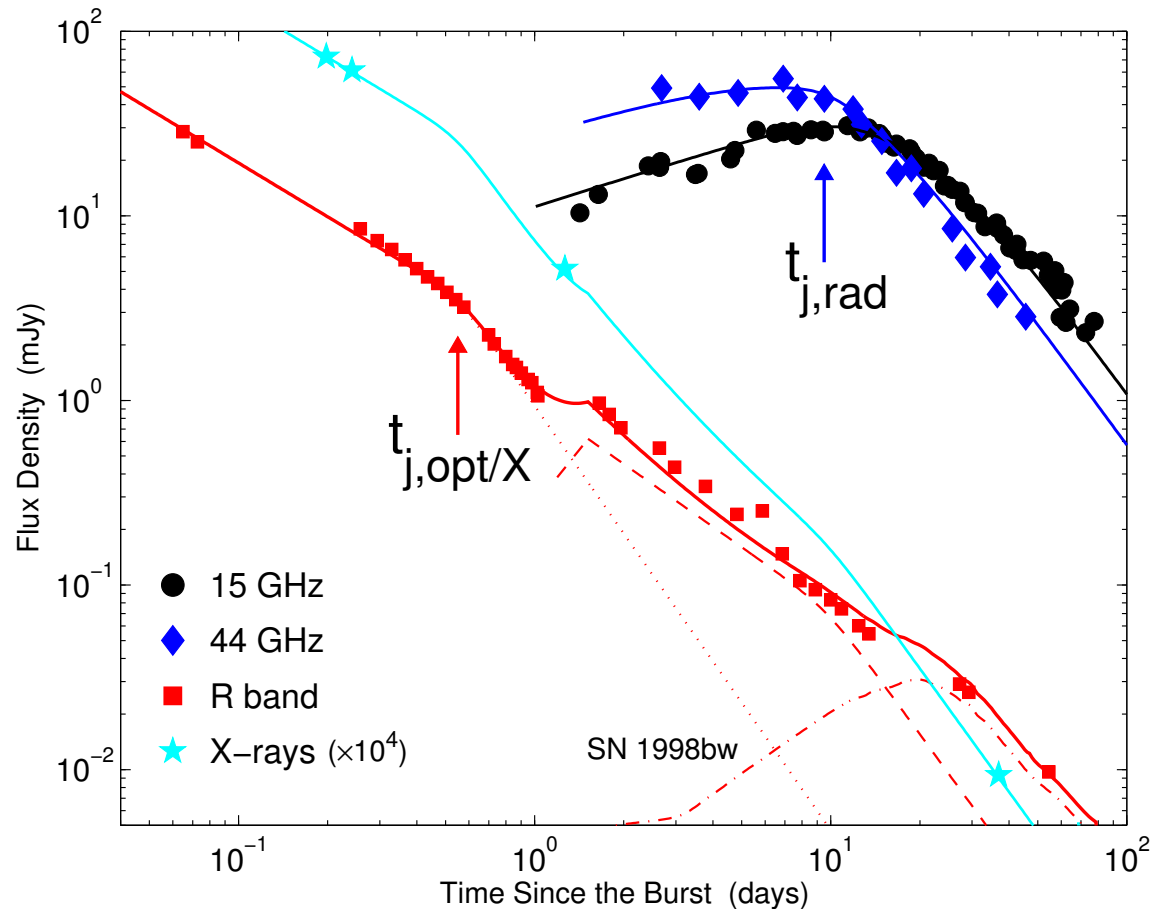
Due to the magnetic collimation $V_{\text{neutron},\perp} \sim 0.1c$ at decoupling.

Thus, **a two component outflow** is naturally created:

- **An inner jet consisting of the protons** (with $\gamma = 200$ and $\mathcal{E}_p = 10^{51}$ ergs).
- The decoupled neutrons, after undergoing β decay at a distance $\sim 4 \times 10^{14}(\gamma_d/15)\text{cm}$, form **a wider proton component** (with $\gamma = 15$ and $\mathcal{E}_p = 2 \times 10^{51}$ ergs).

(See Peng, Königl, & Granot, ApJ (2005) for implications.)

Evidence for two jets!



Radio to X-ray lightcurves of the afterglow of GRB 030329 (Berger et al. 2003).

A two-component jet model provides a reasonable fit to the data.

Conclusion

- Trans-Alfvénic flow:
 - ★ The flow is initially thermally accelerated ($\xi\gamma = \text{const.}$; the magnetic field only guides the flow), and subsequently magnetically accelerated up to Lorentz factors corresponding to equipartition between kinetic and Poynting fluxes, i.e., $\sim 50\%$ of the initial total energy is extracted to baryonic kinetic. $\gamma \propto \varpi$ in both regimes.
 - ★ The fieldline shape is parabolic, $z \propto \varpi^2$ and becomes asymptotically cylindrical.
- Super-Alfvénic flow:
 - ★ Similar results, except that the Lorentz factor increases with lower rate: $\gamma \propto \varpi^\beta, \beta < 1$. Also $z \propto \varpi^{\beta+1}$.
- Neutron decoupling:
 - ★ In pure-hydro case $\gamma_d \sim \gamma_\infty$.
 - ★ Magnetic fields make possible $\gamma_d \ll \gamma_\infty$.
 - ★ The decoupled neutrons decay into protons at a distance $\sim 4 \times 10^{14}(\gamma_d/15)\text{cm}$. In contrast with the situation in the pure-hydro case, these two components are unlikely to interact with each other in the hydromagnetic case since their motions are not collinear.
 - ★ Observational signatures of the neutron component?

The ideal MHD equations

Maxwell:

$$\nabla \cdot \mathbf{B} = 0 = \nabla \times \mathbf{E} + \frac{\partial \mathbf{B}}{c \partial t}, \quad \nabla \times \mathbf{B} = \frac{\partial \mathbf{E}}{c \partial t} + \frac{4\pi}{c} \mathbf{J}, \quad \nabla \cdot \mathbf{E} = \frac{4\pi}{c} J^0$$

Ohm: $\mathbf{E} = \mathbf{B} \times \mathbf{V}/c$

baryon mass conservation (continuity):

$$\frac{d(\gamma \rho_0)}{dt} + \gamma \rho_0 \nabla \cdot \mathbf{V} = 0, \quad \text{where} \quad \frac{d}{dt} = \frac{\partial}{\partial t} + \mathbf{V} \cdot \nabla$$

energy $U_\mu T^{\mu\nu}_{,\nu} = 0$ (or specific entropy conservation, or first law for thermodynamics):

$$\frac{d\left(P/\rho_0^{4/3}\right)}{dt} = 0$$

momentum $T^{\nu i}_{,\nu} = 0$: $\gamma \rho_0 \frac{d(\xi \gamma \mathbf{V})}{dt} = -\nabla P + \frac{J^0 \mathbf{E} + \mathbf{J} \times \mathbf{B}}{c}$

Eliminating t in terms of s : $(\mathbf{V} \cdot \nabla_s) (\xi \gamma \mathbf{V}) - \frac{(\nabla_s \cdot \mathbf{E}) \mathbf{E} + (\nabla_s \times \mathbf{B}) \times \mathbf{B}}{4\pi \gamma \rho_0} + \frac{\nabla P}{\gamma \rho_0} =$

$$(V_p - c) \frac{\partial (\xi \gamma \mathbf{V})}{\partial s} + \frac{\partial (E + B_\phi)}{4\pi \gamma \rho_0 \partial s} \frac{\nabla_s A}{|\nabla_s A|} \times \mathbf{B} - \nabla_s A \frac{\nabla_s \ell \cdot \nabla_s A}{|\nabla_s A|^2} \frac{\partial (E^2 - B_\phi^2)}{8\pi \gamma \rho_0 \partial s}$$